Journal of Luminescence 129 (2009) 1575–1577

Contents lists available at ScienceDirect

Journal of Luminescence

journal homepage: www.elsevier.com/locate/jlumin

Effect of confinement on the Eu^{3+} emission band $^5D_0 \rightarrow {}^7F_0$ in Eu^{3+}-doped nano-glass-ceramics

D. Saurel [a,*], V.K. Tikhomirov [a], V.V. Moshchalkov [a], C. Görller-Walrand [b], K. Driesen [b]

[a] INPAC—Institute for Nanoscale Physics and Chemistry, Katholieke Universiteit Leuven, Belgium
[b] Chemistry Department, Katholieke Universiteit Leuven, Belgium

ARTICLE INFO

Available online 12 June 2009

Keywords:
Glass ceramics
Nanocrystals
Optical properties
Magneto-optical effects
Photoluminescence
Confinement effect

ABSTRACT

We report a non-linear blue shift of the zero-phonon emission line $^5D_0 \rightarrow {}^7F_0$ of Eu^{3+}-dopant in Eu^{3+}-doped nano-glass-ceramics in magnetic field up to 50 T. The shift is significantly larger in nano-glass-ceramics compared to its precursor glass, suggesting that the nanoceraming of the precursor glass decreases the effective mass of the f-electrons bands of Eu^{3+} resulting in their enhanced magnetic confinement. Moreover, the non-linear character of the magnetic field dependence of this blue energy shift denotes a spatial confinement of f-electrons wave-functions of Eu^{3+} dopants in the PbF_2-based nanocrystals of the nano-glass-ceramics where up to 90% of the dopants partition. The spatial confinement seems to be due to an admixture to the f-states of Eu^{3+} of its higher lying states of opposite parity which fall in the quantum well comprising of Eu^{3+}-doped PbF_2 crystalline nanoparticles embedded in the surrounding glass network.

1. Introduction

Transparent nano-glass-ceramics (NGC) $32(SiO_2)9(AlO_{1.5})31.5(CdF_2)18.5:(PbF_2)5.5(ZnF_2)3.5(ReF_3)$, mol% doped with rare-earth (Re) ions such as Er^{3+}, Ho^{3+}, Tm^{3+}, Dy^{3+}, which partition in PbF_2-based crystalline nanoparticles, is a promising medium for efficient infrared emission [1] with a perspective of application in infrared laser and optical amplifier devices [2]. For instance, it has been shown recently that an external magnetic field, by inducing Zeeman split and blue energy shift in the 1.55 μm $^4I_{13/2} \rightarrow {}^4I_{15/2}$ emission band of Er^{3+}-dopant, is a promising option for flattening and broadening the bandwidth of infrared active optical devices based on Er^{3+}-doped NGC [3]. The magnetic field dependence of the blue energy shift of zero-phonon line of the $^4I_{13/2} \rightarrow {}^4I_{15/2}$ band, interpreted as due to magnetic confinement, suggests a spatial confinement effect on f-electron wave-function of Er^{3+} dopant in the PbF_2-based crystalline nanoparticles [3]. Here, we have undertaken a study of magnetic confinement on the $^5D_0 \rightarrow {}^7F_0$ emission band of Eu^{3+}-doped NGC, in magnetic field up to 50 T. The rare-earth ion Eu^{3+} (see energy level diagram in Fig. 1), is known to be the most sensitive probe for rare-earth dopant environment, due to a unique narrow emission band $^5D_0 \rightarrow {}^7F_0$, which does show neither Zeeman nor Stark splitting since the excited $^5D_0$ and ground $^7F_0$ states are non degenerate ($J = 0$) [4–8].

2. Experimental

The synthesis of rare-earth doped NGC, including the Eu^{3+}-doped, has been described elsewhere [1]. A precursor glass (PG) is first synthesized, then it is heat-treated which results in precipitation of spherical PbF_2-based crystalline nanoparticles doped with Eu^{3+}, as found by energy dispersive spectroscopy attachment in a transmission electron microscope (EDS TEM) [1 and refs. therein]. The diameter of Eu^{3+}-doped PbF_2 nanocrystals in NGC has been found to be about 8 ± 1 nm obtained from high-resolution TEM images. The EDS study of the PbF_2-based crystalline nanoparticles indicated that their actual chemical composition is near $Eu_{10}Pb_{25}F_{65}$.

For PL measurements, NGC and PG samples have been prepared with thickness of 0.3 mm and surface area $3 \times 3\,mm^2$. The magnetic field was applied perpendicular to the sample surface area, with PL observed parallel to the applied pulsed magnetic field up to 50 T. The PL spectra have been measured by using an Andor Shamrock 303I spectrometer coupled to an IXON UV–vis em-CCD camera.

3. Results and discussion

Fig. 2 shows the 4.2 K photoluminescence spectra corresponding to the $^5D_0 \rightarrow {}^7F_0$ and $^5D_0 \rightarrow {}^7F_1$ transitions of Eu^{3+}-doped NGC (thick black line) and PG (thin red line) in zero magnetic field. The $^5D_0 \rightarrow {}^7F_0$ electric dipole moment transition is completely forbidden due to selection rules in the theory of the f–f

* Corresponding author.
E-mail addresses: damien.saurel@ensicaen.fr (D. Saurel), victor.tikhomirov@fys.kuleuven.be (V.K. Tikhomirov).

0022-2313/$ - see front matter © 2009 Elsevier B.V. All rights reserved.
doi:10.1016/j.jlumin.2009.04.100

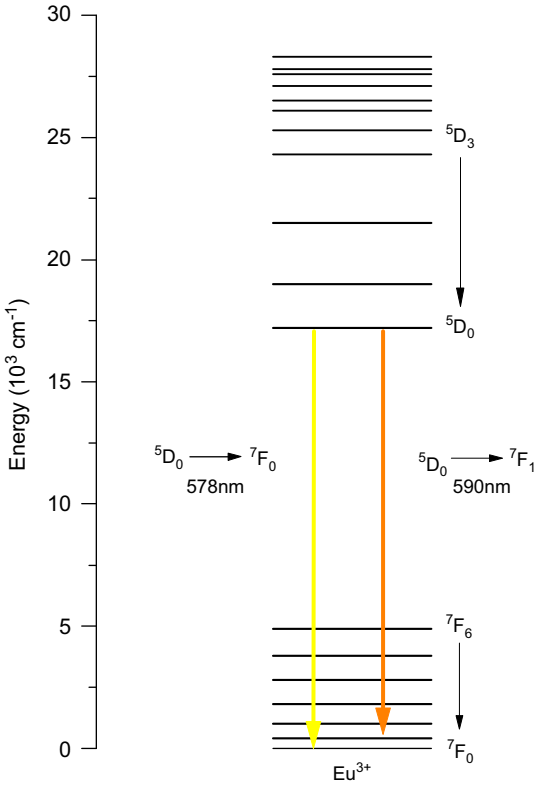

Fig. 1. Energy levels diagram of Eu^{3+}. The studied transitions are indicated by down-headed yellow and orange arrows. Excitation was at 457 nm of Ar^{3+}-laser into $^5D_3$ level. (For interpretation of the references to color in this figure legend, the reader is referred to the web version of this article.)

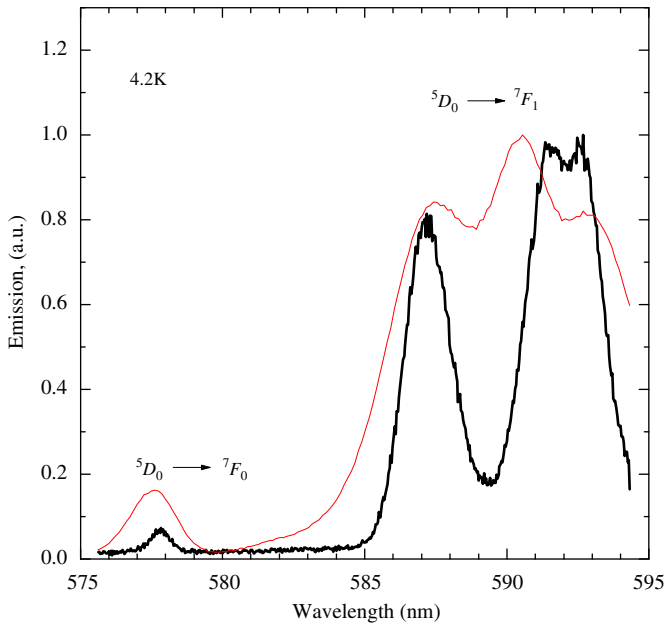

Fig. 2. Emission spectra of 4.2 K of Eu^{3+}-doped GC (thick black line) and precursor glass (thin red line). (For interpretation of the references to color in this figure legend, the reader is referred to the web version of this article.)

transitions in rare-earth ions for both static and vibration-induced perturbations of the parity of the involved levels by the ligand field [7,8]. This transition can only gain small intensity by J–J mixing. As it occurs between non-degenerated energy levels

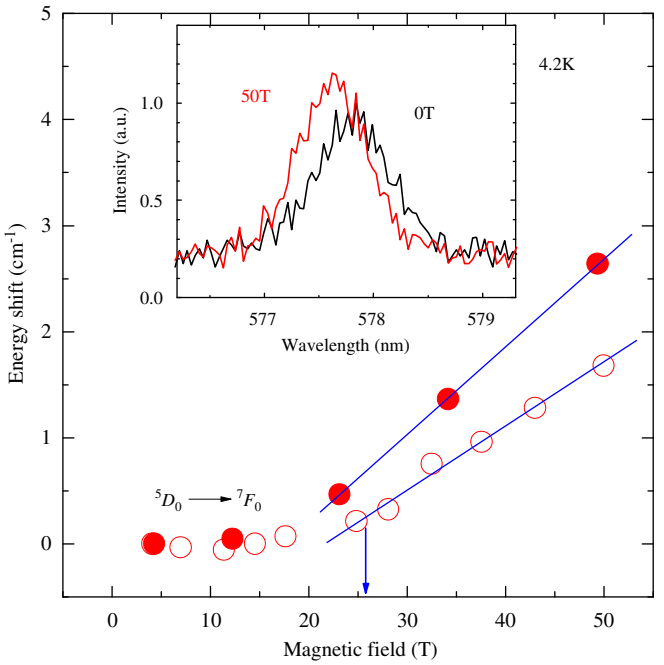

Fig. 3. Magnetic field dependence of the center of mass of the $^5D_0 \rightarrow {}^7F_0$ emission band in NGC (filled circles) and PG (hollow circles). The inset shows the shape $^5D_0 \rightarrow {}^7F_0$ emission band of NGC at 0 T (thick black curve) and at 50 T (thin red curve). (For interpretation of the references to color in this figure legend, the reader is referred to the web version of this article.)

(J = 0) their splitting serves as a probe for the multiplicity of the dopant sites of Eu^{3+}. Since non appreciable splitting of the emission $^5D_0 \rightarrow {}^7F_0$ band is observed (see Fig. 2), we can conclude that the Eu^{3+} site is single in NGC. Moreover, the substantially higher Stark splitting of the $^5D_0 \rightarrow {}^7F_1$ emission band in NGC compared to PG, shows that the Eu^{3+} site in NGC is crystalline [7].

Fig. 3 shows an effect of high magnetic field, up to 50 T, on the $^5D_0 \rightarrow {}^7F_0$ emission band in NGC and PG. As seen in insert of Fig. 3, the $^5D_0 \rightarrow {}^7F_0$ emission band in NGC is clearly shifted to a higher energy when an external magnetic field is applied. A qualitatively similar behavior is observed in PG. The position of the center of mass of this band has been plotted vs. external magnetic field in Fig. 3 for NGC (filled circle) and PG (hollow circle). A linear shift of the peak to higher energy vs. external magnetic field is clearly observed for NGC and PG above 20 T. This linear shift is typical of magnetic confinement effect [9,10], when a strong magnetic field compresses electronic wave-functions in the plane perpendicular to its direction. The gain in energy related to this effect, given by Eq. (1), is inversely proportional to the effective mass μ of the involved electrons/holes.

$$\Delta E = \frac{\hbar e}{2\mu} B \tag{1}$$

It is seen from Fig. 3 that the slope, $\hbar e/2\mu$, according to Eq. (1), of the linear part of the dependence above 25 T is smaller for PG compared to NGC. This suggests that the higher ordering of Eu^{3+} site in NGC results in a smaller effective mass of electrons involved in the $^5D_0 \rightarrow {}^7F_0$ transition.

Moreover, it is seen from Fig. 3 that in the range 0–25 T the dependence of the center of mass vs. external magnetic field is no longer linear. This indicates that magnetic confinement does not play an important role at such values of magnetic field and, therefore, such magnetic field dependence is a signature of spatial confinement effect. It occurs when electronic wave-functions of

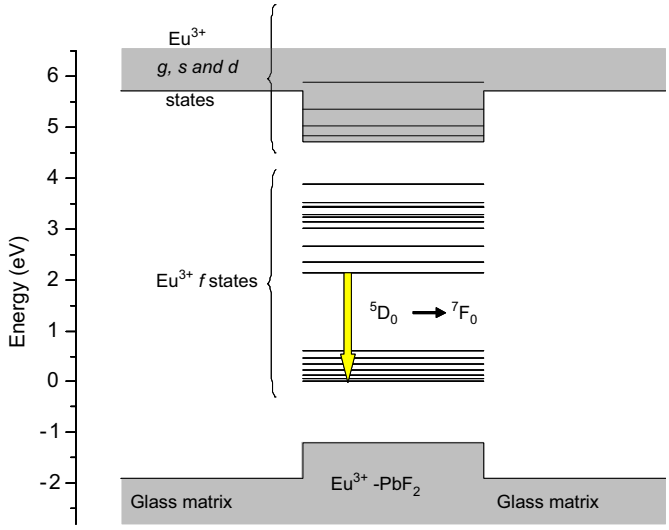

Fig. 4. Schematic representation of energy levels of the Eu^{3+} dopant in quantum well of PbF_2 separated by a barrier from the surrounding glass network.

electrons involved in the $^5D_0 \rightarrow {}^7F_0$ transition are already spatially confined in absence of magnetic field [9,10]. The critical magnetic field B_c at about 25 ± 5 T (indicated by arrow in Fig. 3) corresponds to a crossover from the linear to non-linear (parabolic) dependence. B_c is proportional to the average diameter D of the quantum well, where a spatial confinement occurs, as described by below [9,10]

$$B_c = 2\hbar/eD^2 \quad (2)$$

From Eq. (2), we can estimate the diameter D of the quantum well confining electronic wave-functions to be 6 ± 1 nm. This is similar, within the error bar, to the size 8 ± 1 nm of the PbF_2-based nanocrystals which embed the Eu^{3+} dopant in NGC (see experimental section). This is an interesting result, since wave-function of f-electrons of rare-earth ions are known to have a spatial expansion which is smaller that the size of PbF_2 nanocrystals. Therefore, spatial confinement of f-electrons should arise from admixed higher energy levels of Eu^{3+}, which have a sufficiently larger expansion to experience a confinement.

The optical gap in nanocrystals, which are PbF_2-based [1], is close to $E_g = 5.9$ eV [11] and it is probably smaller than in the surrounding SiO_2–Al_2O_3–CdF_2-based glass network, because it is smaller for each of the components of the glass network (SiO_2 ($E_g = 8.9$ eV [12]), Al_2O_3 ($E_g = 6.24$ eV [13]) and CdF_2 ($E_g = 7.6$ eV [14])). Therefore, the upper-lying g, s or d-states of Eu^{3+} may experience quantum confinement as they are located above 50000 cm^{-1}, i.e. above 6 eV (so-called charge transfer bands of lanthanides [15]), and may fall into the quantum well of PbF_2 crystal separated by a barrier from the surrounding glass network, as illustrated by Fig. 4. Due to an essential admixture of g, s and d-states to f-states of Eu^{3+}, some degree of the quantum confinement can be transferred onto f-states of Er^{3+}.

The dependence of the center of mass of Eu^{3+} $^5D_0 \rightarrow {}^7F_0$ band in PG vs. external magnetic field is reminiscent of NGC, with similar value of the critical magnetic field B_c of 25 ± 5 T. This indicates that nanoceraming of precursor glass, i.e. precipitation of the Eu^{3+}-doped crystalline nanoparticles, occurs by spatial ordering of a similar scale quasi-crystalline "embryos" of the precursor glass.

4. Conclusion

A magnetic field-induced blue energy shift has been detected in the $^5D_0 \rightarrow {}^7F_0$ emission band of Eu^{3+} in nano-glass-ceramics and its precursor glass. The magnetic field dependence of this blue shift changes from parabolic to linear at about 25 T, indicating a spatial confinement of wave-functions of f-electrons of Eu^{3+} mixed with wave-functions of its upper states. The size of the confined wave-function has been calculated from the crossover in the field dependence and it equals to the diameter of crystalline nanoparticles hosting Eu^{3+}. In precursor glass, the magnetic field dependence of the energy shift is reminiscent of that in nano-glass-ceramics, indicating that during the nanoceraming of precursor glass, the synthesis of Eu^{3+}-doped crystalline nanoparticles PbF_2 occurs by spatial ordering of a similar scale quasi-crystalline "embryos" of the precursor glass. The magnetic field dependence above 25 T indicates the blue energy shift is linear with applied magnetic field, with a slope significantly larger in the nano-glass-ceramics. This suggests that the nanoceraming results in lowering the effective mass of f-electrons of Eu^{3+}.

Acknowledgements

The support from the Flemish Science Fund (FWO), the K.U. Leuven Concerted Action Scheme (GOA), the IAP network of the Belgian Government, the FP6-SANDiE, the FP6-EuroMagNET (RII3-506239) and the KULeuven center of excellence INPAC are greatly acknowledged.

References

[1] V.K. Tikhomirov, D. Furniss, I.M. Reaney, M. Beggiora, M. Montagna, R. Rolli, Appl. Phys. Lett. 81 (2002) 1937.
[2] P.C. Becker, N.A. Olsson, J.R. Simpson, Erbium-Doped Fibre Amplifiers: Fundamentals and Technology, Academic, San Diego, 1999.
[3] D. Saurel, V.K. Tikhomirov, V.V. Moshchalkov, C. Görller-Walrand, K. Driesen, Appl. Phys. Lett. 92 (2008) 171101.
[4] M.J. Weber, in: W.M. Yen, P.M. Meltzer (Eds.), Laser Spectroscopy of Solids, Vol. 49, Springer, Berlin, 1986, p. 189.
[5] J. Méndez-Ramos, V. Lavín, I.R. Martín, U.R. Rodríguez-Mendoza, V.D. Rodríguez, A.D. Lozano-Gorrín, P. Núnez, J. Appl. Phys. 94 (2003) 2295.
[6] C. Liu, Y.W. Hong, J. Heo, J. Non-Cryst. Solids 351 (2005) 2317.
[7] K. Driesen, V.K. Tikhomirov, C. Görller-Walrand, J. Appl. Phys. 102 (2007) 024312.
[8] C. Görller-Walrand, K. Binnemans, in: K.A. Gschneidner Jr., L. Eyring (Eds.), Handbook on the Physics and Chemistry of Rare Earths, Vol. 25, Elsevier, Amsterdam, The Netherlands, 1998, p. 101.
[9] R. Provoost, M. Hayne, M.K. Zundel, K. Eberl, V.V. Moshchalkov, Physica B 258 (1998) 203;
Y. Sidor, B. Partoens, F.M. Peeters, N. Schildermans, M. Hayne, V.V. Moshchalkov, A. Rastelly, O.G. Schmidt, Phys. Rev. B 73 (2006) 155334.
[10] P.D. Wang, J.L. Merz, S. Fafard, R. Leon, D. Leonard, G. Medeiros-Ribeiro, M. Oestreich, P.M. Petroff, K. Uchida, N. Miura, H. Akiyama, H. Sakaki, Phys. Rev. B 53 (1996) 16458;
K.L. Janssens, F.M. Peeters, V.A. Schweigert, Phys. Rev. B 63 (2001) 205311.
[11] H. Jiang, R. Orlando, M.A. Blanco, R. Pandey, J. Phys. Condens. Matter 16 (2004) 3081;
I. Kosacki, J.M. Langer, Phys. Rev. B 33 (1986) 5972.
[12] R.B. Laughlin, Phys. Rev. B 22 (1980) 3021.
[13] S. Mo, W.Y. Ching, Phys. Rev. B 57 (1998) 15219.
[14] A.S. Shcheulin, D.E. Onopko, A.I. Ryskin, Phys. Solid State 39 (1997) 1906.
[15] P. Dorenbos, J. Phys.: Condens. Matter 15 (2003) 8417.